Dowel Bar Optimization: Phases I and II

Final Report

Sponsored by American Highway Technology

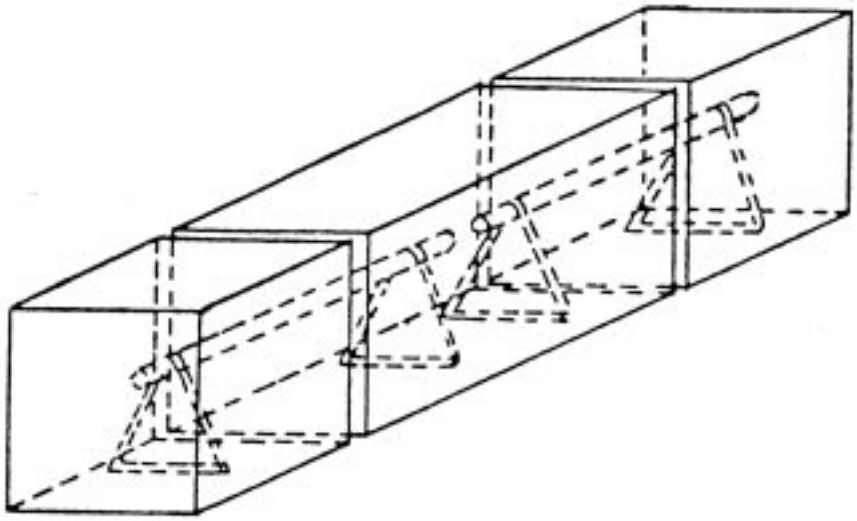

Center for Transportation Research and Education

Center for Portland Cement Concrete Pavement Technology

Department of Civil and Construction Engineering

Iowa State University

October 2001

CTRE's mission is to develop and implement innovative methods, materials, and technologies for improving transportation efficiency, safety, and reliability while improving the learning environment of students, faculty, and staff in transportation-related fields.

DOWEL BAR OPTIMIZATION: PHASES I AND II

FINAL REPORT

Principal Investigator
Max L. Porter
Professor of Civil and Construction Engineering, Iowa State University

Research Assistants
Robert J. Guinn, Jr.
Andrew L. Lundy

Preparation of this report was financed in part
through funds provided by American Highway Technology

Center for Transportation Research and Education
Center for Portland Cement Concrete Pavement Technology
Iowa State University
Iowa State University Research Park
2901 South Loop Drive, Suite 3100
Ames, IA 50011-8632
Telephone: 515-294-8103
Fax: 515-294-0467
http://www.ctre.iastate.edu

OCTOBER 2001

TABLE OF CONTENTS

1 INTRODUCTION 1
1.1 Background 1
1.2 Experimental and Analytical Investigation 2
1.2.1 Objective 2
1.2.2 Scope 3
1.3 Literature Review 3

2 ACCOMPLISHMENTS TO DATE 5
2.1 Phase I: Elemental Static Direct Shear Testing 5
2.1.1 Introduction 5
2.1.2 Analytical Theory of Dowel Bars 7
2.1.3 Direct Shear Testing Procedure 11
2.2 Phase II: Bar Spacing 14
2.2.1 Introduction 14
2.2.2 Dowel Bar Load Distribution 14

3 RESULTS 18
3.1 Introduction 18
3.2 Specimen Failure 18
3.3 Determination of K_o 19
3.4 Dowel Bar Spacing 22

4 CONCLUSIONS AND RECOMMENDATIONS 26
4.1 Conclusions 26
4.2 Recommendations 27
4.2.1 Load Transfer Efficiency 27
4.2.2 AASHTO Test Modifications 27

5 CONTINUING WORK: PHASES III AND IV 29
5.1 Phase III: Full-Scale Laboratory Setup 29
5.2 Phase IV: Field Test 29

ACKNOWLEDGMENTS 30

REFERENCES 31

APPENDIX A: RELATIVE DEFLECTION VERSUS LOAD DIAGRAMS

APPENDIX B: K_O VERSUS Y_O GRAPHS

LIST OF FIGURES

Figure 2.1 Elemental Fatigue Specimen (*4*) 6
Figure 2.2 Relative Deflection Between Adjacent Pavement Slabs (*9*) 10
Figure 2.3 Location of Load on Specimen (*11*) 12
Figure 2.4 Deflection versus Load Diagram for the 1-1/2"ϕ Epoxy-Coated Steel Dowel Bars in Specimen 3 13
Figure 2.5 Load Transfer Distribution Proposed by (a) Friberg and (b) Tabatabaie et al. (*9*) 17
Figure 3.1 K_o versus y_o for the 1-1/2"ϕ Round Epoxy-Coated Steel Dowel Bar 21
Figure 3.2 Worst Possible Load Case for Dowel Bar Spacing 23

LIST OF TABLES

Table 2.1 Test Matrix of AASHTO T253 Specimens 6
Table 3.1 Test Matrix of the Specimens Taken to Failure..... 18
Table 3.2 Load at Which Failure Occurred for Specimen 19
Table 3.3 Average Relative, Shear, and Face of the Joint Deflections..... 20
Table 3.4 Average Modulus of Dowel Support and Concrete Bearing Stress..... 22
Table 3.5 Dowel Bar Spacing and Associated Relative Deflection (in.)..... 25
Table 3.6 Allowable Bearing Stress and Bearing Stress (psi) at Associated Dowel Spacing 25

1 INTRODUCTION

1.1 Background

America's roadways are in serious need of repair. According to the American Society of Civil Engineers (ASCE), one-third of the nation's roads are in poor or mediocre condition (*1*). ASCE has estimated that under these circumstances American drivers will sacrifice $5.8 billion and as many as 13,800 fatalities a year from 1999 to 2001 (*1*). A large factor in the deterioration of these roads is a result of how well the steel reinforcement transfers loads across the concrete slabs. Fabricating this reinforcement using a shape conducive to transferring these loads will help to aid in minimizing roadway damage.

Load transfer within a series of concrete slabs takes place across the joints. For a typical concrete paved road, these joints are approximately 1/8-inch gaps between two adjacent slabs. Dowel bars are located at these joints and used to transfer load from one slab to its adjacent slabs. As long as the dowel bar is completely surrounded by concrete no problems will occur. However, when the hole starts to oblong a void space is created and difficulties can arise. This void space is formed due to a stress concentration where the dowel contacts the concrete. Over time, the repeated process of traffic traveling over the joint crushes the concrete surrounding the dowel bar and causes a void in the concrete. This void inhibits the dowel's ability to effectively transfer load across the joint. Furthermore, this void gives water and other particles a place to collect that will eventually corrode and potentially bind or lock the joint so that no thermal expansion is allowed. Once there is no longer load transferred across the joint, the load is transferred to the foundation and differential settlement of the adjacent slabs will occur.

Differential settlement of the slabs creates a roughness at the joints, making vehicle travel uncomfortable and requiring that the slab be repaired or replaced.

As was mentioned in the previous paragraph, a void around a dowel bar is formed by stress concentrations crushing the concrete directly in contact with the dowel. When a shear load is applied to the concrete slab, the force is supported only by the top or bottom of the dowel bar, not the sides. Since the stress concentration region lies on the top or bottom of the dowel bar, the smaller the dowel the higher the stress concentration. The sides of the dowel bar do not aid in the distribution of the shear load from the concrete. Therefore, the size of the top and bottom of the dowel bar is where the stress concentration is located and is directly related to the width and/or shape of the dowel bar. While round dowel bars handle these stress concentrations relatively well, elliptical bars provide more area for the stresses to distribute onto.

1.2 Experimental and Analytical Investigation

Before a change can even be considered, contractors, engineers, owners, and manufacturers want to be certain that a new product or procedure will yield beneficial results when compared to the current method of construction. The following research was conducted in order to compare the static performance of steel elliptical dowel bars to that of epoxy-coated dowel bars, which are currently in use today. Research was also done on the effect that dowel bar spacing has on the performance of concrete pavements.

1.2.1 Objective

The objectives of Phases I and II were

1. to investigate the static behavior of steel elliptical and round epoxy-coated dowel bars,
2. to investigate the failure modes of steel elliptical and round epoxy-coated dowel bars,

3. to evaluate the benefits and drawbacks of elliptically shaped dowels bars for load transfer,
4. to determine the effect of dowel bar spacing and projected load transfer efficiency, and
5. to evaluate if variable spacing in combination with shape factor and bar size can optimize costs and constructability.

The main objective of this research was to determine which dowel bar and spacing should be used for the testing during Phase III, a full-scale accelerated laboratory test.

1.2.2 Scope

The scope of Phases I and II included

1. construction of elemental specimens for static direct shear testing of steel elliptical and round epoxy-coated dowel bars,
2. testing of elemental specimens under direct shear loading,
3. analyzing results from direct shear tests to determine the modulus of dowel support, K_o,
4. analyzing results using K_o to determine the concrete bearing stress at the face of the joint, σ_b,
5. compiling all available information on dowel bar spacing, and
6. analyzing the effect of dowel bar spacing on concrete pavements.

1.3 Literature Review

The literature review included theoretical modeling of dowel bars, highway pavement dowel bars, and bar spacing. A discussion and use of the references can be found throughout the report. The appropriate references can be found under the discussion of the associated topic. The references section at the end of this report contains the significant references used in this report. A more complete list of references is contained in reports prepared for the Iowa Department of

Transportation; see HR-325 from May 1992 (*2*), HR-343 from November 1993 (*3*), and TR-408 from January 1999 (*4*).

2 ACCOMPLISHMENTS TO DATE

2.1 Phase I: Elemental Static Direct Shear Testing

2.1.1 Introduction

The elemental direct shear test provides a means to monitor the deflection across a joint of a dowel bar embedded in concrete. The purpose of this research is to determine the modulus of dowel support, K_o, for the steel elliptical and round epoxy-coated dowel bars. Once K_o is determined it will be used to determine the concrete bearing stress at the face of the joint, σ_b. Once the bearing stress is known the dowel bars can be compared to determine which type of dowel bar applies the lowest stress to the concrete. In this project there were five different types of dowel bars tested. Ten dowel bars of each dowel bar type were used. Two dowel bars were placed in each specimen, which required the construction of 25 concrete specimens. The different types of dowel bars were as follows:

- 1-1/4"ϕ epoxy-coated steel
    - area = 1.227 in^2
- 1-1/2"ϕ epoxy-coated steel
    - area = 1.767 in^2
- large elliptical steel (major axis = 1.98 in., minor axis = 1.34 in.)
    - area = 2.084 in^2
- medium elliptical steel (major axis = 1.66 in., minor axis = 1.13 in.)
    - area = 1.473 in^2
- small elliptical steel (major axis = 1.41 in., minor axis = 0.88 in.)
    - area = 0.975 in^2

See Table 2.1 for a test matrix of the specimens tested.

Table 2.1 Test Matrix of AASHTO T253 Specimens

Description of Dowel Bar	Number of Test Specimens	Number of Dowel Bars
1-1/4”ϕ epoxy-coated steel	5	10
1-1/2”ϕ epoxy-coated steel	5	10
Large elliptical steel	5	10
Medium elliptical steel	5	10
Small elliptical steel	5	10

The specimens were formed using prefabricated steel forms. The elemental specimens were constructed as a modified American Association of State Highway and Transportation Officials (AASHTO) T253 specimen (*5*) with the same dimensions as the specimen shown in Figure 2.1. This specimen size was used to represent a 12-inch thick slab. A 1/8-inch gap was used to simulate a field pavement as well as aid in the reduction of flexure across the joint.

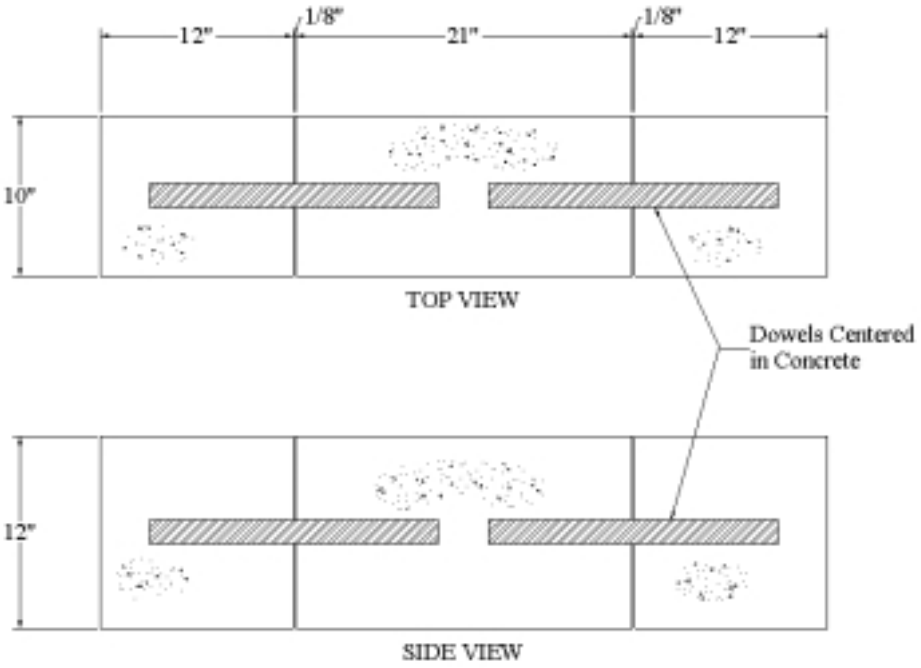

Figure 2.1 Elemental Fatigue Specimen (*4*)

As can be seen in Figure 2.1, the dowel bars were placed at midheight of the specimen. The elliptical dowel bars were oriented with the long dimension, or major axis, parallel to the ground. This orientation was chosen so the elliptical dowel bars provided a larger width for the

concrete to bear against than that of a round bar with a similar cross-sectional area. The benefits of the larger bearing width will be explained in greater detail in the next section.

2.1.2 Analytical Theory of Dowel Bars

2.1.2.1 Analytical Model

Timoshenko and Lessels worked on the first model of a beam on an elastic foundation that could be applied to a dowel bar system (*6*). According to Timoshenko, the deflection of a beam on an elastic foundation is found using Equation 2.1:

$$EI\frac{d^4y}{dx^4} = -ky \qquad (2.1)$$

where k is a constant usually called the modulus of foundation and y is the deflection. The modulus of foundation denotes the reaction per unit length when the deflection is set equal to one.

The solution to Timoshenko's differential equation is found in Equation 2.2.

$$y = e^{\beta x}(A\cos\beta x + B\sin\beta x) + e^{-\beta x}(C\cos\beta x + D\sin\beta x) \qquad (2.2)$$

where

$\beta = \sqrt[4]{k/4EI}$ = relative stiffness of the beam on the elastic foundation (in^{-1})
k = modulus of foundation (psi)
E = modulus of elasticity of the dowel (psi)
I = moment of inertia of the dowel (in^4)

By applying the appropriate boundary conditions for the problem the constants A, B, C, and D can be solved. For a semi-infinite beam with a moment, M_o, and a point load, P, Equation 2.2 is equivalent to Equation 2.3.

$$y = \frac{e^{-\beta x}}{2\beta^3 EI}[\mathrm{P}\cos\beta\mathrm{x} - \beta M_o(\cos\beta x - \sin\beta x)] \quad (2.3)$$

Friberg applied Timoshenko's elastic foundation theory to a beam of semi-infinite length (*7*). When trying to calculate the deflection at the face of the joint, it can be determined by setting x = 0 in Equation 2.3. This equation then becomes Equation 2.4.

$$\mathrm{y_o} = \frac{\mathrm{P_t}}{4\beta^3 \mathrm{EI}}(2 + \beta \mathrm{z}) \quad (2.4)$$

where

$$\beta = \sqrt[4]{\frac{\mathrm{K_o b}}{4\mathrm{EI}}} = \text{relative stiffness of the dowel bar encased in concrete (in.}^{-1}\text{)} \quad (2.5)$$

K_o = modulus of dowel support (pci)
b = dowel bar width (in.)
E = modulus of elasticity of the dowel bar (psi)
I = moment of inertia of the dowel bar (in^4)
P_t = load transferred through the dowel bar (lb.)
z = joint width (in.)

Friberg used the modulus of dowel support, K_o, in his equation. The modulus of dowel support is the reaction per unit area causing a deflection equal to one. Friberg used the expression $K_o b$ to replace the modulus of foundation, k, from Timoshenko's model. Friberg's equation was developed using a semi-infinite dowel length. Dowel bars have a finite length so this equation would not apply to dowel bars used in practice today. However, Porter et al. have shown that Friberg's equation can be used with little to no error if the βL value is greater than two (*2*, *8*). Where the length, L, is taken to be the length of the dowel bar embedded in concrete, or approximately one-half the dowel bar length.

2.1.2.2 Relative Deflection across a Pavement Joint

The relative deflection across a pavement joint consists of four separate components. These components, as shown in Figure 2.2, consist of the deflection of the dowel at each joint face, the deflection due to the slope of the dowel bar, shear deflection, and flexural deflection. When considering all possible components for relative deflection the following expression in Equation 2.6 is found.

$$\Delta = 2y_o + z\left(\frac{dy_o}{dx}\right) + \delta + \frac{P_t z^3}{12EI} \tag{2.6}$$

where

y_o = deflection at the face of the joint

$$\delta = \frac{\lambda P_t z}{AG} = \text{shear deflection} \tag{2.7}$$

P_t = load transferred by dowel bar (lb.)
λ = form factor, equal to 10/9 for solid circular sections and ellipses
A = cross-sectional area of the dowel bar (in^2)
G = shear modulus (psi)

In this research a joint width of 1/8 inches was used for the specimens. Using such a small joint width allows the deflection due to the slope of the dowel bar to be approximately equal to zero, which is the case in the authors' research since the width and the slope of the joint are small. This small joint width also means that the flexural deflection is approximately equal to zero since the joint width term is cubed. After removing both the slope and flexural deflections from Equation 2.6, Equation 2.8 remains.

$$\Delta = 2y_o + \delta \tag{2.8}$$

Solving Equation 2.8 for y_o yields Equation 2.9.

$$y_o = \frac{\Delta - \delta}{2} \tag{2.9}$$

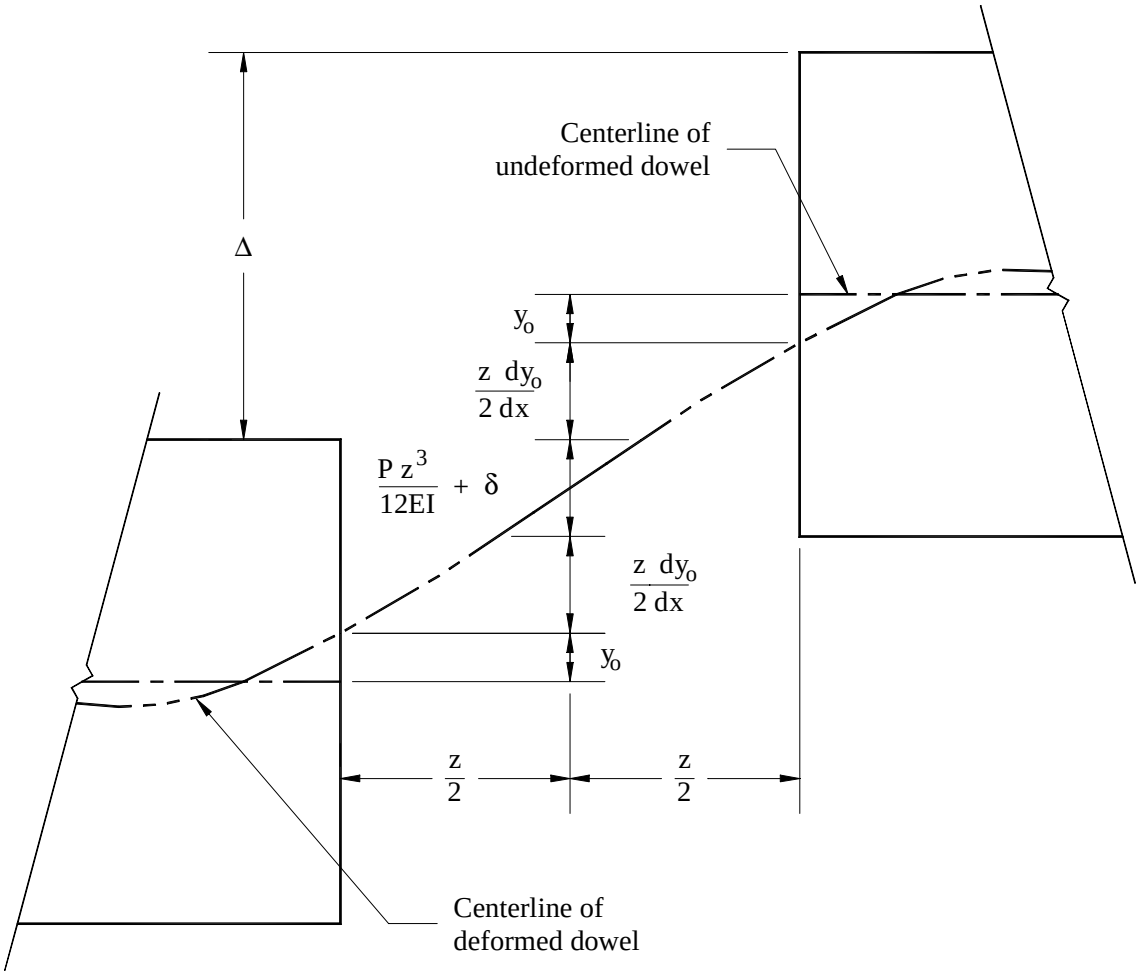

Figure 2.2 Relative Deflection Between Adjacent Pavement Slabs (*9*)

2.1.2.3 Bearing Stress of Dowel Bars in Concrete

The bearing stress on the concrete at the face of the joint is critical for proper function of the dowel bar in the concrete. If the bearing stress on the concrete becomes too large the concrete will begin to break away where it contacts the dowel bar. Repetitive high-stress loadings of the dowel bar-concrete interface will create a void. This void creates an additional amount of deflection in the system before the dowel bar will begin to take on the load applied. This

additional deflection creates a loss in the efficiency of the dowel bar to transfer load across the joint. This loss in efficiency must now be carried by the subgrade, which puts additional stress on the subgrade and creates the possibility for differential settlement of adjacent slabs.

If the dowel behaves as a beam on an elastic foundation, the bearing stress at the face of the joint, σ_b, is proportional to the deflection at the face of the joint. This relationship is expressed using Equation 2.10.

$$\sigma_b = K_o y_o \qquad (2.10)$$

The bearing stress on the concrete needs to be kept low to make certain that no crushing of the concrete occurs. According to the American Concrete Institute's (ACI) Committee 325, the allowable bearing stress on the concrete is equivalent to Equation 2.11 (*10*).

$$\sigma_a = \left(\frac{4-b}{3}\right) f'_c \qquad (2.11)$$

where

σ_a = allowable bearing stress (psi)
b = dowel bar width (in.)
f'_c = compressive strength of concrete (psi)

This equation provides a factor of safety of approximately three.

2.1.3 Direct Shear Testing Procedure

The testing of the specimens was conducted on a 400-kip capacity SATEC 400HVL universal testing machine at the Iowa State University structures laboratory. A modified AASHTO T253-76 test was used for testing the elemental direct shear specimens. This procedure requires that the end blocks of the specimens be clamped so that no rotation is allowed. With the end blocks restrained from rotation, a load of 2000 lb./min. was applied to the middle section of the specimen while deflections were measured. Figure 2.3 shows how the load was applied to the center section of the specimen. The deflections that were measured were the

relative deflections across the joint, or rather the deflections from the stationary end blocks to the deflecting center block. The deflections were measured by using Direct Current Displacement Transducers (DCDTs). Measurements of deflection and corresponding load were taken every two seconds. Before testing began, the specimens were preloaded. The preloading procedure consisted of loading the specimens five times at a rate of 2000 lb./min. until 5,000 lb. was reached. This procedure was used to help settle the specimens so that more accurate results would be obtained. The tests were carried out on all specimens until a load of 10,000 lb. was reached. This data were then used to create a load versus deflection diagram, as seen in Figure 2.4. This procedure has been tested and validated as an acceptable approach by Rohner (*11*). Load versus deflection diagrams for all the dowel bars are displayed in Appendix A.

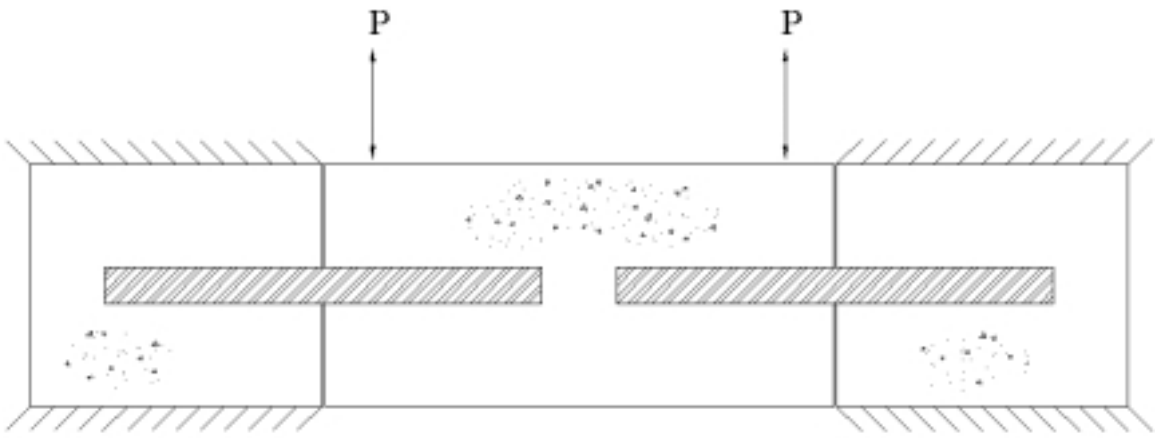

Figure 2.3 Location of Load on Specimen (*11*)

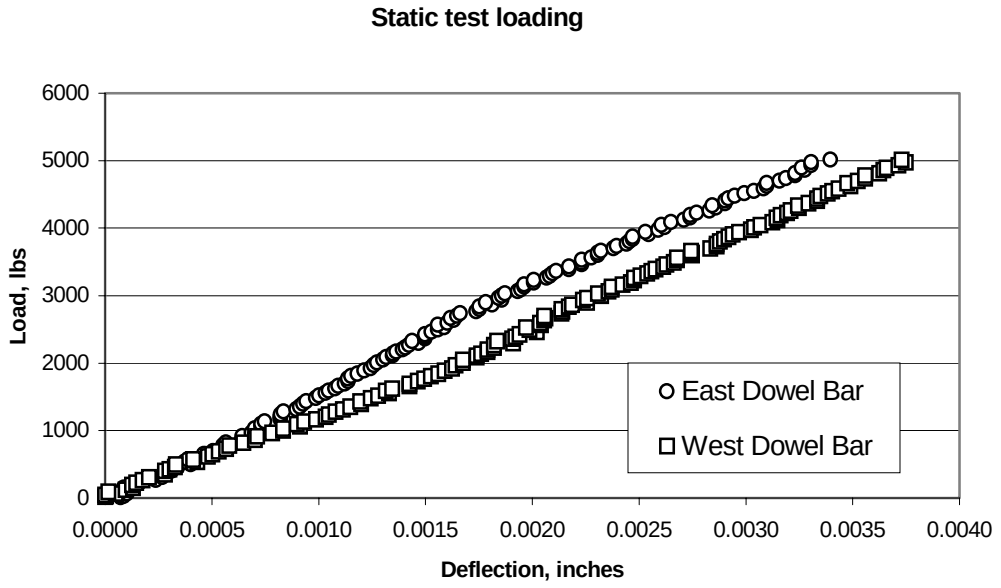

Figure 2.4 Deflection versus Load Diagram for the 1-1/2"ϕ Epoxy-Coated Steel Dowel Bars in Specimen 3

While testing the first two specimens, a problem was encountered. While preparing the initial specimens for testing, the authors observed that the specimens were not sitting level in the testing apparatus. The decision was made to conduct the first tests and attach two DCDTs to the rear of both end blocks. The end block DCDTs were mounted to measure the movement of the end blocks opposite the dowel bars, or to check the end blocks for rotation. After performing tests on the first two specimens, the DCDTs revealed that there was a significant amount of rotation occurring on the end blocks.

This rotation was due to the unevenness of the bottom of the specimens. The forms used to cast the specimens were not perfectly flat, which created unevenness along the bottom of the specimen. This unevenness on the bottom of the specimens caused them to sit unevenly. As load was applied movement of the end blocks would occur. The solution to this problem was to cast the bottom of the end blocks in dental plaster. The plaster that was used for this procedure was Labstone, which had a compressive strength of 8000 psi. Upon retests of the two initial

specimens the rotation was again monitored and no measurable amount of rotation was seen. All the remaining specimens were cast in the Labstone to be sure that the bottoms remained level during testing. As a precaution rotation readings were taking for all the specimens to ensure that no rotation occurred on any of the remaining specimen.

2.2 Phase II: Bar Spacing

2.2.1 Introduction

When slabs are of the same dimensions and are subjected to equal loads, the spacing of the dowel bars will determine how much load each dowel bar is subjected to. The larger the spacing between the dowel bars, the greater the loads applied to the dowel bars will be due to the distribution of loads through the concrete and subgrade.

2.2.2 Dowel Bar Load Distribution

In an ideal situation, when a load is placed near a joint, the dowel bars would assume half the load and the remaining load is transferred to subgrade. However, no joint will behave in this ideal manner because of the repeated loadings seen by a pavement joint. This repetitive loading will create a small void and some load transfer efficiency of the dowel bar will be lost. According to Ioannides and Korovesis this efficiency can be determined by calculating the transferred load efficiency (TLE) in Equation 2.12 (*12*).

$$TLE = \frac{P_t}{P_w} \times 100\% \qquad (2.12)$$

where

TLE = transferred load efficiency (%)
P_t = load transferred across the joint (lb.)
P_w = applied wheel load (lb.)

The maximum value for the transferred load efficiency is 50 percent. Brown and Bartholomew stated that for heavy truck traffic, a TLE ranging from 35 to 40 percent is considered acceptable (*13*).

Yoder and Witczak suggested a 5–10 percent decrease in load transfer across a joint due to the void that appears after repetitive loadings (*14*). Allowing a conservative five percent decrease in load transfer yields Equation 2.13.

$$P_t = 0.45P_w \tag{2.13}$$

where

P_t = load transferred across the joint (lb.)
P_w = applied wheel load (lb.)

When a wheel load is applied near a joint, not all dowel bars at the joint aid in transferring the load. The dowel bars closest to the applied wheel load transfer more of the load than the dowel bars furthest away from the applied load. Friberg was the first to investigate the load distribution to the dowel bars across a joint (*7*). Based on an analysis by Westergaard, Friberg proposed that dowel bars contained outside $1.8l_r$ from the applied load were ineffective in transferring any additional load, where l_r is the radius of relative stiffness as shown in Equation 2.14 (*15*).

$$l_r = \sqrt[4]{\frac{E_c h^3}{12(1-\mu^2)K}} \tag{2.14}$$

where

l_r = radius of relative stiffness (in.)
E_c = modulus of elasticity of the pavement concrete (psi)
h = pavement thickness (in.)
μ = Poisson's ratio for the concrete pavement
K = modulus of subgrade reaction (pci)

Friberg also believed that a linear distribution of load occurred inside the radius of relative stiffness as shown in Figure 2.5. Friberg's analysis was based on dowel bars having a diameter of

0.75 or 0.875 inches and with dowel bar spacing ranging from 12 to 20 inches. If a larger dowel bar is used or the bar spacing is less than 12 inches, then Friberg's model no longer applies.

Since Friberg's model is not useful for the construction practices used today, another model was required. Tabatabaie et al. modeled a doweled joint using finite element and were able to show that an effective length of $1.0l_r$ is more appropriate for today's construction practices (*16*). Tabatabaie was also able to show that a linear approximation does exist with the maximum shear occurring beneath the applied load itself. For dowel bar design, a calculation of the maximum shear load is useful and will be referred to as the load seen by the critical dowel bar, P_c.

Since Tabatabaie was able to show a linear relationship with the load distribution along the joint, the load seen by the critical dowel bar, P_c, can now be calculated. The first step is to draw a triangle with a base that extends out a distance $1.0l_r$ in both directions from where the load is applied and has a peak height directly below the applied load, as shown in Figure 2.5. For simplicity, set the height of the triangle below the load equal to one P_c. Using the linear relationship of the load distribution along the joint, calculate the height of the triangle below each dowel bar. Sum up the heights below all of the dowel bars to determine the number of effective dowels, N_{eff}, that are used in transferring the applied load. The shear force that is directly beneath the applied load can now be calculated using Equation 2.15.

$$P_c = \frac{P_t}{N_{eff}} \qquad (2.15)$$

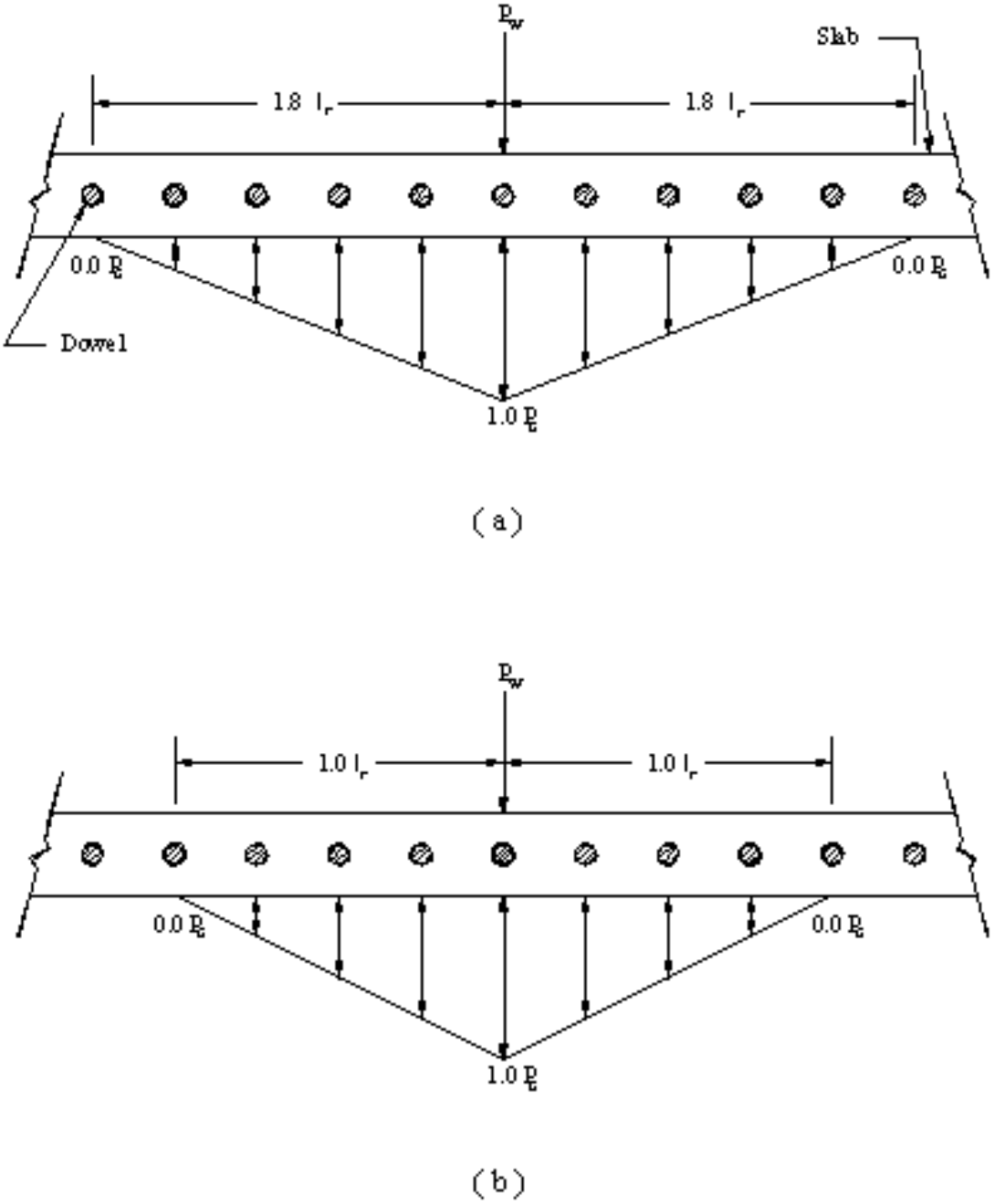

Figure 2.5 Load Transfer Distribution Proposed by (a) Friberg and (b) Tabatabaie et al. (*9*)

3 RESULTS

3.1 Introduction

All the specimens listed in Section 2.1.1 were tested using the elemental direct shear test that was outlined in Section 2.1.3. The elemental direct shear tests provide a way to experimentally determine a deflection versus load diagram. With the deflection versus load diagram, the modulus of dowel support, $K_{o,}$ can be determined using the theoretical formulas outlined previously by Friberg. Once a value for the modulus of dowel support has been determined, the concrete bearing stress, σ_b, can be calculated. The concrete bearing stress is the measure of the stress applied at the dowel bar-concrete interface and is a good indicator to the longevity of the concrete system. The method for determining the modulus of dowel support and the concrete bearing stress will be outlined in greater detail later.

3.2 Specimen Failure

After all 25 specimens had been tested and a deflection versus load diagram was constructed for each dowel bar, 10 of the specimens were tested to failure. The 10 specimens tested to failure consisted of two specimens of each type of dowel bar. Two of the five specimens from each dowel bar type were chosen at random for the testing. Table 3.1 lists the test matrix of the specimens taken to failure.

Table 3.1 Test Matrix of the Specimens Taken to Failure

Description of Dowel Bar	Number of Test Specimens	Number of Dowel Bars
1-1/4”ϕ epoxy-coated steel	2	4
1-1/2”ϕ epoxy-coated steel	2	4
Large elliptical steel	2	4
Medium elliptical steel	2	4
Small elliptical steel	2	4

Each specimen was placed into the SATEC test machine and a load of 2000 lb./min. was applied until failure of the specimen. Table 3.2 lists each specimen type and the average load at which failure occurred.

Table 3.2 Load at Which Failure Occurred for Specimen

Description of Dowel Bar inside Specimen	Average Failure Load of Specimen (lb.)
1-1/4"ϕ epoxy-coated steel	35,795
1-1/2"ϕ epoxy-coated steel	43,315
Large elliptical steel	45,760
Medium elliptical steel	38,775
Small elliptical steel	38,545

As can be seen in Table 3.2, the failures occurred following a trend. As the cross-sectional area of the dowel bar increases so does the applied failure load. However, the small elliptical dowel bars do not properly follow this trend. This difference is attributable to only having tested two specimens. It is possible to have one beam skew the results, as appears to be the case with the small elliptical dowel bars. One of the small elliptical dowel bar specimens failed at a load that would have followed the trend. However, the second specimen did not fail until a much greater load. The second specimen skewed the average upward and forced the small elliptical dowel bars away from the trend. The authors believe that if more specimens were tested and used in the determination of the average failure load the trend would become even more pronounced.

3.3 Determination of K_o

As mentioned previously, the first step in determining the modulus of dowel support, K_o, was to develop a load-deflection relationship for each specimen. This was done with the data collected during the elemental direct shear test using linear regression to develop a direct relationship between load and deflection. With this relationship determined the total relative

deflection for a given load could then be calculated. The load that was chosen in this research was 2000 lb. This load was chosen for two reasons:

1. This would be approximately the highest load that a dowel bar could see with any regularity, according to our highest dowel bar spacing.
2. Since there is a linear relationship between load and deflection the results for the modulus of dowel support do not depend on the load (*11*).

With the relative deflection calculated for the specified load, the next step is to calculate the deflection at the face of the joint using Equation 2.7 and Equation 2.9 for shear deflection, δ, and deflection at the face of the joint, y_o, respectively. Both of these equations are repeated here for convenience.

$$\delta = \frac{\lambda P_t z}{AG} \tag{2.7}$$

$$y_o = \frac{\Delta - \delta}{2} \tag{2.9}$$

The average relative deflection, shear deflection, and average deflection at the face of the joint are shown in Table 3.3.

Table 3.3 Average Relative, Shear, and Face of the Joint Deflections

Dowel Bar Description	Average Relative Deflection, Δ (in.)*	Shear Deflection, δ (in.)*	Average Deflection at Face of Joint, y_o (in.)*
1-1/4”ϕ epoxy-coated steel	0.002642	0.000020	0.001311
1-1/2”ϕ epoxy-coated steel	0.001642	0.000014	0.000814
Large elliptical steel	0.001968	0.000012	0.000978
Medium elliptical steel	0.002432	0.000017	0.001207
Small elliptical steel	0.002383	0.000025	0.001179

*Note: The deflections cannot be measured this accurately but are needed to display the effects of shear deflection.

The last step required to calculate the modulus of dowel support was to create a graph of the modulus of dowel support versus deflection at the face of the joint. By imputing the geometric properties for the dowel bar and substituting multiple values of K_o into the theoretical equation the deflection at the face of the joint was determined. Equations 2.4 and 2.5 are required to complete the K_o versus y_o graph as discussed earlier and are repeated here for convenience.

$$y_o = \frac{P_t}{4\beta^3 EI}(2+\beta z) \qquad (2.4)$$

$$\beta = \sqrt[4]{\frac{K_o b}{4EI}} \qquad (2.5)$$

As can be seen in Equation 2.4, listed above, the value of y_o is dependant on the shape of the dowel bar. Therefore, for every dowel bar type a separate K_o versus y_o graph must be generated. In Figure 3.1 a sample K_o versus y_o graph is shown, the graph shown is for a 1-1/2"ϕ round epoxy-coated steel dowel bar calculated at a 2,000-lb. load. The K_o versus y_o graphs for all the dowel bar types are displayed in Appendix B.

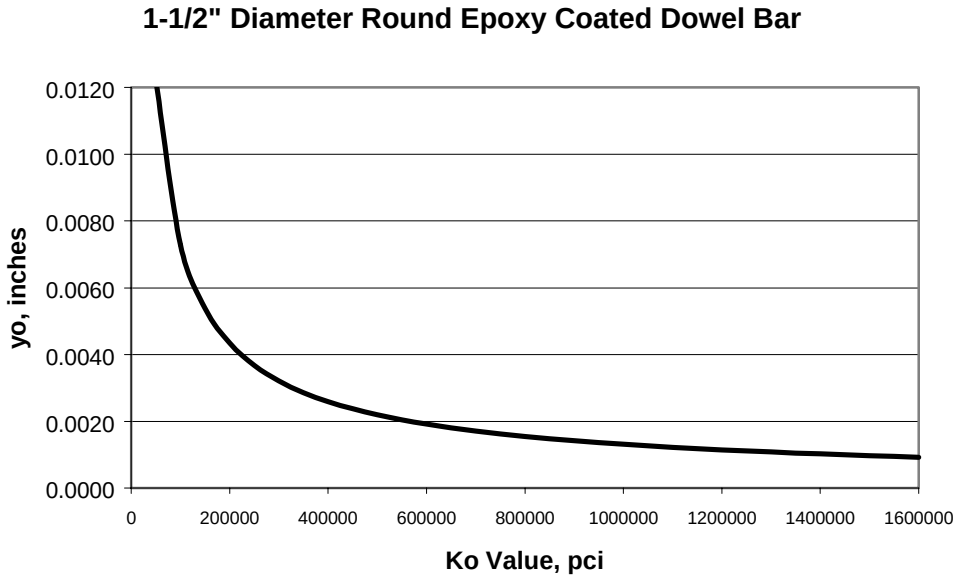

Figure 3.1 K_o versus y_o for the 1-1/2"ϕ Round Epoxy-Coated Steel Dowel Bar

Using the modulus of dowel support and the deflection at the face of the joint, the concrete bearing stress can be calculated. Again, this equation is repeated here for convenience.

$$\sigma_b = K_o y_o \qquad (2.10)$$

Table 3.4 is a listing of each specimen type and its associated average modulus of dowel support and average concrete bearing stress at a load of 2,000 lb.

Table 3.4 Average Modulus of Dowel Support and Concrete Bearing Stress

Dowel Bar Description	Modulus of Dowel Support, K_o (pci)	Concrete Bearing Stress, σ_b (psi)
1-1/4"ϕ epoxy-coated steel	1,796,654	2,084
1-1/2"ϕ epoxy-coated steel	2,092,820	1,568
Large elliptical steel	1,319,621	1,147
Medium elliptical steel	1,492,246	1,611
Small elliptical steel	2,473,999	2,637

3.4 Dowel Bar Spacing

There are two approaches that can be followed to arrive at the appropriate dowel bar spacing. The design approach differs on the determining factor that is used to calculate the dowel bar spacing. The two options for designing dowel bar spacing are as follows:

1. The bearing stress on the concrete can be set equal to the allowable bearing stress.
2. The relative deflection of the joint can be set not to exceed to a maximum value.

When using the allowable bearing stress method to determine the bar spacing, the bearing stress was not the controlling factor in the design of spacing with steel bars. Designing using the allowable bearing stress allowed the spacing of the bars to become larger than that which would be practical. In this case, the bearing stress not being the controlling factor makes sense due to the fact that the allowable bearing stress is for the crushing of the concrete. The allowable bearing stress should not be approached if the dowel bars are to have useful field life.

For the reasons above the choice was made to design the dowel bar spacing based on the acceptable relative deflection. To simplify the discussion of relative deflection, Table 3.5 was created to compare several dowel bars spacings and the associated relative deflection for a 12-inch-thick slab.

Note that the spacing was calculated by determining the worst possible load case for P_c. P_c was calculated using Equation 2.15 as discussed previously, which is repeated here for convenience.

$$P_c = \frac{P_t}{N_{eff}} \qquad (2.15)$$

The worst load case for P_c is when the wheel load of the car is placed directly over the outermost dowel bar in the pavement. In this particular load case there are only dowel bars located on one side of the wheel load; see Figure 3.2. This situation significantly reduces the number of dowel bars that can effectively transmit load; in other words N_{eff} is decreased to its smallest possible value. As can be seen by Equation 2.15, with N_{eff} at its minimum value, then P_c would be at its maximum value.

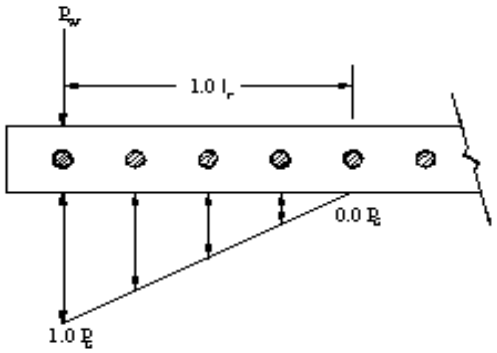

Figure 3.2 Worst Possible Load Case for Dowel Bar Spacing

Table 3.6 lists the bearing stress along with the allowable bearing stress for a 12-inch-thick slab with the same load and dowel bar spacing that was used in Table 3.5.

As can be seen in Tables 3.5 and 3.6, in every spacing situation the elliptical dowel bars reduce the bearing stress when they are compared to a round dowel bar with a similar cross-sectional area. When comparing the 1-1/2”ϕ round epoxy-coated steel dowel bars to the large elliptical steel dowel bars, the large elliptical steel dowel bars produce bearing stresses on the concrete that are greatly reduced while the increase in relative deflection is minimal. The large elliptical steel dowel bars have an increase in cross-sectional area of nearly 18 percent but provide a reduction in bearing stress of 26 percent. In contrast, the 1-1/2”ϕ round epoxy-coated steel dowel bars have a 44 percent increase in cross-sectional area yet only provide a 25 percent reduction in bearing stress when compared to the 1-1/4”ϕ round epoxy-coated steel dowel bars.

Table 3.5 Dowel Bar Spacing and Associated Relative Deflection (in.)

Dowel Bar Description	Spacing of Dowel Bars, Center to Center (in.)						
	20	18	16	14	12	10	8
1-1/4”ϕ round epoxy-coated steel	0.0026	0.0025	0.0023	0.0020	0.0018	0.0016	0.0013
1-1/2”ϕ round epoxy-coated steel	0.0017	0.0016	0.0015	0.0013	0.0012	0.0010	0.0008
Large elliptical steel	0.0020	0.0018	0.0017	0.0015	0.0013	0.0012	0.0010
Medium elliptical steel	0.0024	0.0023	0.0021	0.0019	0.0017	0.0015	0.0012
Small elliptical steel	0.0024	0.0023	0.0021	0.0019	0.0017	0.0014	0.0012

Table 3.6 Allowable Bearing Stress and Bearing Stress (psi) at Associated Dowel Spacing

Dowel Bar Description	σ_a (psi)	Spacing of Dowel Bars, Center to Center (in.)						
		20	18	16	14	12	10	8
1-1/4”ϕ round epoxy-coated steel	6,142	2,329	2,190	2,020	1,804	1,601	1,390	1,143
1-1/2”ϕ round epoxy-coated steel	5,583	1,752	1,648	1,519	1,357	1,204	1,046	860
Large elliptical steel	4,511	1,286	1,209	1,115	996	884	767	631
Medium elliptical steel	5,226	1,808	1,700	1,567	1,400	1,243	1,079	887
Small elliptical steel	5,784	2,955	2,779	2,562	2,288	2,031	1,763	1,450

4 CONCLUSIONS AND RECOMMENDATIONS

4.1 Conclusions

The results of this research indicated that the elliptical dowel bars behaved as predicted. When comparing the 1-1/2”ϕ round epoxy-coated steel dowel bars to the large elliptical steel dowel bars, the large elliptical steel dowel bars produce bearing stresses on the concrete that are greatly reduced while the increase in relative deflection is minimal. The large elliptical steel dowel bars have an increase in cross-sectional area of nearly 18 percent but provide a reduction in bearing stress of over 26 percent. In contrast, the 1-1/2”ϕ round epoxy-coated steel dowel bars have a 44 percent increase in cross-sectional area over the smaller 1-1/4”ϕ round epoxy-coated steel dowel bars yet only provide a 25 percent reduction in bearing stress. The round dowel bars did retain a slight advantage in the stiffness over elliptical dowel bars of a similar cross-sectional area due to their shape. However, this difference in stiffness is insignificant based on the small variance in the deflection of the slabs. The difference in magnitude of the deflections is so small that the dowel bars could be considered as having roughly the same deflection.

This research has shown that the 1.5”ϕ round epoxy-coated steel dowel bars have roughly same bearing stress as the medium elliptical dowel steel bars. This occurrence could be beneficial if the load transfer efficiency was determined.

Dowel bar spacing is a method to distribute load to the dowel bars. The smaller the spacing of the dowel bars the smaller the load on the dowel bars. A decrease in pavement thickness will lower the number of bars available for load transfer, and a smaller spacing may be required. Poor subgrade material will also decrease the number of dowel bars available for load transfer, and therefore a smaller spacing may also be needed.

4.2 Recommendations

4.2.1 Load Transfer Efficiency

The authors recommend that a series of tests be conducted to determine the load transfer efficiency of the dowel bars. Past research has indicated that the lower the bearing stresses on the concrete the less efficient the dowel bars were at transferring load. In the load transfer testing the large and medium elliptical steel dowel bars should be compared with the 1-1/2”ϕ round epoxy-coated steel dowel bars. The medium elliptical steel dowel bar would be ideal to compare to the 1-1/2”ϕ round epoxy-coated steel dowel bars since both bars have approximately the same bearing stress on the concrete. By comparing these two bars it may be possible to make a determination of which dowel bar shape transfers load better. The large elliptical steel dowel bars should also be included in the comparison to see how they relate in load transfer efficiency.

The dowel bar spacing is dependant on the thickness of the pavement if similar subgrade and loading conditions exist. For most pavements a 12-inch spacing would be sufficient for today’s traffic loads. If the pavement thickness is reduced or an unsuitable subgrade is used then the spacing may need to be decreased to compensate.

The three dowel bars listed above should be used in the Phase III full-scale testing. The results of Phase III will be used to make a determination as to the bar that will be used in Phase IV. The best dowel bar for Phase IV would have the best load transfer efficiency combined with the lowest bearing stress. Phase III and IV should also be done with the elliptical bars having an epoxy coating since this is how they would be manufactured when released to the market for corrosion protection.

4.2.2 AASHTO Test Modifications

The authors believe that modifications to the current Load-Deflection Test Procedure portion of the AASHTO T253 test should be made. Many methods and qualifications for the

current test procedure are outdated or inadequate for today's standards. The following are proposed modifications to the Load-Deflection Test Procedure portion of AASHTO T253:

- The specimens should be molded with a 1/8-inch gap in between sections, as in accordance with standard practice, as opposed to the test methods recommended 3/8-inch gap. Provisions are needed (as well as parameter studies) for the effects of various gap widths.
- Specimen dimensions should be changed according to pavement thickness.
- The ends of the specimen should be held down well enough in order to prevent rotation and instrumentation should be stipulated to monitor possible rotation.
- The bottom sides of the specimen need to be cast in plaster in order to be flush with the testing machine.
- An amount of allowable end rotation needs to be determined as to not void the test results.
- A new applied load rate and higher applied load need to be determined in order to construct better deflection versus load diagrams.
- A new maximum allowable deflection across the joint should be determined for design.
- The specimen should be loaded using point loads located at the ends of the interior section and not uniformly, pending inflection point investigation.

Updating this test will yield results more suitable to field application and allow different dowel bars to be compared. By modifying this test, a universal procedure may be used in order to determine and evaluate K_o and the concrete bearing stress underneath any dowel bar.

5 CONTINUING WORK: PHASES III AND IV

5.1 Phase III: Full-Scale Laboratory Setup

The next step in this research is to perform accelerated tests on pavement sections in a laboratory setting. The results found herein, from Phases I and II, will help provide guidance on many decisions in the next phase of research. The primary purpose of the full-scale laboratory testing is to determine how efficient the dowel bars recommended in this research are at transferring load. Phase III will also allow researchers to check the fatigue behavior of the elliptically shaped dowel bars, since this was not in the scope of the work in Phases I or II.

The results of Phase III will be used to recommend the optimum dowel bar shape, size, and spacing that will be used in the field test, Phase IV.

5.2 Phase IV: Field Test

The final phase in this research will be to place an agreed upon dowel bar in a roadway around central Iowa. This will be the first opportunity to try out these elliptically shaped dowel bars in a field situation. The dowel bars will be monitored over a predetermined length of time and their performance will be evaluated and compared to a control group of 1-1/2”ϕ epoxy-coated steel dowel bars that will simultaneously be placed in the field.

ACKNOWLEDGMENTS

The research described herein was conducted at the Iowa State University Structural Engineering Laboratories in the Department of Civil and Construction Engineering through the auspices of the Center for Transportation Research and Education (CTRE) and the Center for Portland Cement Concrete Pavement (PCC Center) with funds by American Highway Technology.

The authors would like to thank all of those involved for their efforts, but special thanks are given to Mr. Steven L. Tritsch and Dr. Jim Cable, who provided support through their expertise and knowledge toward the project. The authors wish to thank Mr. Dale Harrington, director of the PCC Center, for his project administration leadership.

The authors wish to recognize and thank Dayton Superior of Parsons, Kansas, for providing materials.

The authors would also like to acknowledge the support provided by Mr. Douglas L. Wood, supervisor of the structural engineering laboratory at Iowa State University, for his expertise and assistance.

REFERENCES

1. American Society of Civil Engineers. New Report Card Reveals Little Improvement in Infrastructure. *Civil Engineering*, Vol. 71, No. 4, April 2001, p. 30.

2. Porter, M.L., M. Alberston, B. Barnes, E. Lorenz, and K. Viswanath. *Thermoset Composite Concrete Reinforcement.* Report HR-325. Iowa Department of Transportation and Iowa Highway Research Board, Ames, Iowa, May 1992.

3. Porter, M.L., B. Barnes, B. Hughes, and K. Viswanath. *Non-Corrosive Tie Reinforcing and Dowel Bars for Highway Pavement Slabs.* Report HR-343. Iowa Department of Transportation and Iowa Highway Research Board, Ames, Iowa, Nov. 1993.

4. Porter, M.L., D. Davis, and J. Rohner. *Investigation of Glass Fiber Composite Dowel Bars for Highway Pavement Slabs.* Progress Report TR-408. Iowa Department of Transportation and Iowa Highway Research Board, Ames, Iowa, Jan. 1999.

5. American Standard for Testing and Materials (ASTM). *Annual Book of ASTM Standards.* ASTM, Pa., 1986.

6. Timoshenko, S., and J.M. Lessels. *Applied Elasticity*. Westinghouse Technical Night School Press, Pa., 1925.

7. Friberg, B.F. Design of Dowels in Transverse Joints of Concrete Pavements. *Transactions, American Society of Civil Engineers*, Vol. 105, No. 2081, 1940.

8. Albertson, M.D. *Fibercomposite and Steel Pavement Dowels.* Masters Thesis. Iowa State University, 1992.

9. Davis, D.D. *Fatigue Behavior of Glass Fiber Reinforced Polymer Dowels.* Masters Thesis. Iowa State University, 2001.

10. American Concrete Institute (ACI) Committee 325. Structural Design Considerations for Pavement Joints. *Journal of the American Concrete Institute*, Vol. 28, No. 1, July 1956, pp. 1–28.

11. Rohner, J.G. *Investigation of the Modulus of Dowel Support in Concrete Pavements.* Masters Thesis. Iowa State University, 1999.

12. Ioannides, A.M., and G.T. Korovesis. Analysis and Design of Doweled Slab-on-Grade Pavement Systems. *Journal of Transportation Engineering*, Vol. 118, No. 6, Nov./Dec. 1992, pp. 745–768.

13. Brown, V.L., and C.L. Bartholomew. FRP Dowel Bars in Reinforced Concrete Pavements. *Proceedings of the International Symposium on FRP Reinforcement for Concrete Structures*. American Concrete Institute, Mich., 1993.

14. Yoder, E.J., and M.W. Witczak. *Principles of Pavement Design*. 2nd ed. John Wiley & Sons, Inc., New York, 1975.

15. Westergaard, H.M. Computation of Stresses in Concrete Roads. *Proceedings of the 5th Annual Meeting of the Highway Research Board*. Washington, D.C., 1925.

16. Tabatabaie, A.M., E.J. Barenburg, and R.E. Smith. *Longitudinal Joint Systems in Slipformed Rigid Pavements: Volume II–Analysis of Load Transfer Systems for Concrete Pavements.* Report No. DOT/FAA.RD-79/4. Federal Aviation Administration, U.S. Department of Transportation, Washington, D.C., 1979.